

Constricting force of filamentary protein rings evaluated from experimental results

I. Hörger,¹ F. Campelo,² A. Hernández-Machado,³ and P. Tarazona¹

¹*Departamento de Física Teórica de la Materia Condensada, Universidad Autónoma de Madrid, E-28049 Madrid, Spain*

²*Cell and Developmental Biology Programme, Centre de Regulació Genòmica, E-08003 Barcelona, Spain*

³*Departament d'Estructura i Constituents de la Matèria, Universitat de Barcelona, E-08028 Barcelona, Spain*

(Received 4 August 2009; revised manuscript received 14 January 2010; published 26 March 2010)

We present a model of Z-ring constriction in bacteria based on different experimental *in vitro* results. The forces produced by the Z ring due to lateral attraction of its constituent parts, estimated in previous studies that were based on FtsZ filaments observed by atomic force microscopy, are in good agreement with an estimation of the force required for recently found deformations in liposomes caused by FtsZ. These forces are calculated within the usual Helfrich energy formalism. In this context, we also explain the apparent attraction of multiple Z rings in the liposomes initially separated by small distances, as well as the stable distribution of rings separated by distances greater than approximately twice the diameter of the cylindrical liposomes. We adapted the model to the *in vivo* conditions imposed by the bacterial cell wall, concluding that the proposed mechanism gives a qualitative explanation for the force generation during bacterial division.

DOI: [10.1103/PhysRevE.81.031922](https://doi.org/10.1103/PhysRevE.81.031922)

PACS number(s): 87.17.-d, 87.10.-e, 87.15.-v, 87.16.-b

I. INTRODUCTION

There is a rapidly increasing interest in the biophysical mechanisms for the formation and function of the septal or Z ring needed for cell division of rodlike bacteria [1–8]. The major component of that structure is a filament forming protein called FtsZ, a tubulin homolog in prokaryotic cells. There is a running controversy on what the essential aspects of the protein-protein and protein-membrane interactions responsible for the formation of the Z ring and its constricting action on the membrane are [9]. Different theoretical models have been developed to explore the effects of a Z ring, condensed by the effect of the lateral attractions between the protein filaments, on a cylindrical membrane. Some models [4–7] assume that the radial constricting forces emanate directly from the same lateral attractions that stabilize the ring, while other models [2,3] assume the effects of a spontaneous curvature of the filaments.

A recent experimental study of deformation of cylindrical liposomes under the action of a modified FtsZ protein [10] offers the opportunity to calibrate the possible effects of a Z-ring *in vitro*. Liposomes, made of phospholipid multilamellar structures, were brought in contact with FtsZ-mts, a modified protein with an amphipathic helix to be directly attached to the phospholipid membranes. The result was the formation of tubular liposomes with FtsZ-mts inside. The addition of the polymerizing agent GTP produced the self-assembly of FtsZ-mts rings, attached to the inner side of the lamellar tubes, and associated to weak indentations of the membrane. The relevance of that experiment comes from the highly simplified composition of the *in vitro* system. It makes clear that, when anchored to the phospholipid membrane, FtsZ alone may self-assemble into ring structures and create the constricting force needed to initiate cell constriction. In this paper, we estimate the radial force needed to produce the observed deformations and we compare it with predictions [4,11] based on a very different set of *in vitro* experiments [12], in which FtsZ filaments adsorbed on mica were observed by atomic force microscopy (AFM). Under

the planar geometry imposed by the mica substrate, the filaments form characteristic rolled structures, which were reproduced in Langevin simulations of a theoretical model [4] as a result of the lateral attractions between filaments. The strength of these attractions was estimated from the aspect of the planar rolls and transferred to similar simulations on cylindrical geometry. The results showed that the condensation of the filaments produced by their lateral interactions may produce ring structures and lead to constricting forces in the range of 50–100 pN [11]. The main question we address in this paper is whether or not the observed constrictions of the tubular liposomes in Ref. [10] could be produced by forces of similar strength. The theoretical analysis presented here provides an interpretation for the observed deformations of the liposomes, and we also analyze the implications for the *in vivo* function of the Z ring.

II. MATHEMATICAL MODEL

In the *in vitro* experiments by Osawa *et al.* [10], the multilamellar vesicles are reported to be almost spherical before the insertion of FtsZ. The anchoring of the FtsZ-mts, still without the polymerizing agent GTP, produces tubular shapes that we assume to be the results of a spontaneous curvature H_0 induced by the anchored amphipathic tails of the protein. Within the usual Helfrich Hamiltonian [13], the membrane free energy is written in terms of surface tension, σ , and bending rigidity, κ , contributions,

$$F_{mem} = \int dA \left[\frac{\kappa}{2} (H - H_0)^2 + \sigma \right], \quad (1)$$

where H is the total curvature and dA is the infinitesimal area element. The minimization of F_{mem} with respect to the radius of the cylindrical lamellar tubes, links the observed (equilibrium) radius $R_0 \approx 1.8 \mu\text{m}$ to the unknown parameters σ , κ , and H_0 in Eq. (1), through the relation $R_0^{-2} = H_0^2 + 2\sigma/\kappa$.

The addition of GTP produces the formation of FtsZ filaments and, according to the interpretation of the AFM ex-

periments [4,5,14], the lateral attractive interactions produce Z-ring condensation. Z rings are observed in Ref. [10] through a fluorescent dye and they appear associated to a deformation of the tubular shapes, which we describe here mathematically as a function, $R(z)$, where the z coordinate is taken along the cylindrical axis and axial symmetry is assumed. The ring position, r , corresponds to $z=0$ so that the boundary conditions are $R(0)=R_r$ and $R(z)\rightarrow R_0$ for large $|z|$. The contribution of the Z ring to the free energy is represented by

$$F_r = \oint dl \tau_L, \quad (2)$$

i.e., a line tension, τ_L associated to the ring of FtsZ filaments, and integrated over the transverse section of the tubular membrane. The constricting radial force exerted by the Z ring on the membrane is $f_r = \partial F_r / \partial R_r = 2\pi\tau_L$, and the main aim of this work is to estimate the required value of this force to produce the observed deformation of the cylindrical liposomes in Ref. [10]. From the technical point of view, τ_L can be considered as a Lagrange multiplier, to be determined by the value of R_r (see Appendix A).

III. RESULTS AND DISCUSSION

Within a linear analysis for the deformation, $U(z)=1-R(z)/R_0$, the minimization of the membrane free energy outside the Z ring is given by the solution of

$$\frac{\partial^4 U(\tilde{z})}{\partial \tilde{z}^4} + 2R_0 H_0 \frac{\partial^2 U(\tilde{z})}{\partial \tilde{z}^2} + U(\tilde{z}) = 0, \quad (3)$$

with $\tilde{z}=z/R_0$. Taking the limit of vanishing ring width, the boundary conditions and the symmetry $U(-\tilde{z})=U(\tilde{z})$ are satisfied with $2U'''(0)=-\tau_L R_0/\kappa$ and the obvious symmetry $U(-\tilde{z})=U(\tilde{z})$, where all the derivatives are taken with respect to the dimensionless variable \tilde{z} . The solution of Eq. (3) subject to the boundary conditions $U(\tilde{z})\rightarrow 0$ for large $|\tilde{z}|$ and $U(0)=\Delta \equiv (R_0 - R_r)/R_0$ is given by

$$U(\tilde{z}) = \frac{\Delta \exp(-\zeta^+ |\tilde{z}|)}{\cos(\varphi_0)} \cos(\zeta^+ |\tilde{z}| - \varphi_0), \quad (4)$$

where $\zeta^\pm = \sqrt{(1 \pm R_0 H_0)/2}$ and $\tan(\varphi_0) = \zeta^- / \zeta^+$. Notice that $R_0 H_0$ varies between 0 and 1, depending on the relative importance of surface tension and spontaneous curvature, but we have no experimental access to these parameters. The thickness of the multilamellar membrane in Ref. [10] is about that of 100–200 phospholipid bilayers; therefore, assuming a contribution of 20 kT from the bending rigidity of each bilayer, we could estimate $\kappa \approx 10^{-17}$ J. The surface tension of the tubular liposomes with equilibrium radius $R_0 \approx 1.8$ μm should be $\sigma \leq \kappa / (2R_0^2) \approx 10^{-6}$ N/m, i.e., about ten nanoNewton per meter from each bilayer. The actual value of σ has to be between that upper limit and the null surface tension expected for fully relaxed free standing tubular structures. Under the disordered conditions of the observed tubular structures it is reasonable to accept a wide distribution of σ values between these two limits, which

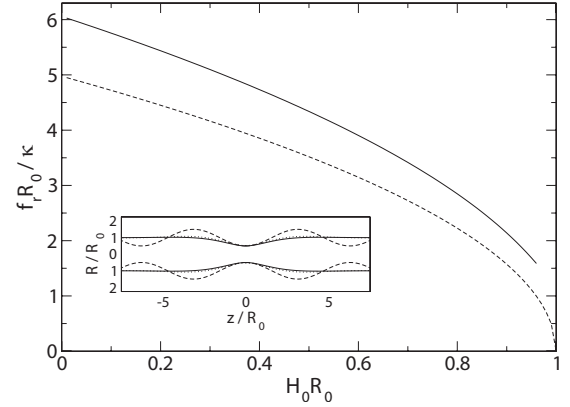


FIG. 1. Force required for a relative deformation $\Delta=0.28$ of a liposome with relative spontaneous curvature $H_0 R_0$. The dashed line is the result of the linear approximation [Eq. (5)], and the continuous line gives an upper bound with nonlinear effects. The inset represents the shape of the deformed membrane for $H_0 R_0=0$ (continuous line), $H_0 R_0=0.5$ (dashed line), and $H_0 R_0=1$ (dotted line).

means a wide distribution of $R_0 H_0$ values, between 0 (for maximum σ) and 1 (for $\sigma=0$), at different portions of the liposome. The generic shape of the deformation Eq. (4) is that of a damped oscillation between the limits shown in Fig. 1 and only in the strict $\sigma=0$ limit ($R_0 H_0=1$) the oscillations in $U(z)$ become undamped, as a pearling instability of the cylindrical shape.

The family of predicted shapes (Fig. 1) is in good qualitative agreement with the microscopy images of multilamellar liposomes presented in Ref. [10] for maximum relative deformation $\Delta \sim 0.2-0.3$. Figure 4 in Ref. [10] shows that the membrane radius next to a constriction exceeds the equilibrium radius although the resolution of the experimental images does not allow the observation of a full period of the membrane deformation. Moreover, the quantitative estimation of $R_0 H_0$ is limited by the dispersion in the deformation shapes found in these images, probably because of the uncontrolled boundary conditions and different local conditions of the tubular liposomes. An experimentally testable consequence of the damped oscillatory deformations [Eq. (4)] induced by a force ring comes from the interaction between different protein rings, periodically distributed along a tubular liposome (see Appendix B). Within the linear approximation [Eq. (3)] the deformation is a superposition of the shifted damped oscillations [Eq. (4)]. We estimate the leading-order (Δ^2) contribution to the free energy as a function of the ring separation z , and the stability with respect to the collapse of neighbor rings. The results in Fig. 2 show that Z-rings self-assembled at large relative distance are stable, keeping similar distances between neighbors along the row. However, rings initially set at a distance shorter than $\approx 5R_0$ would collapse until they leave a sparser periodic distribution. This theoretical prediction is in good agreement with the experimental observations shown in Ref. [10], where Z rings initially formed at distances $|z| \approx 1-2$ μm collapse after 100–200 s, to let an apparently stable distribution of rings separated by 4–6 μm .

Within the linear approximation [Eq. (3)], the radial force exerted by the Z ring on the membrane is given by

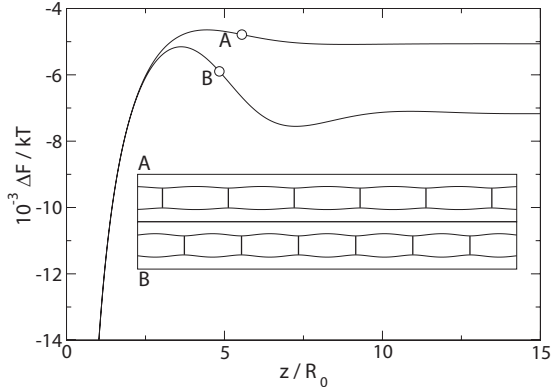


FIG. 2. Free-energy change in a liposome membrane with a periodic distribution of Z rings as a function of the ring separations, (a) $H_0 R_0 = 0$ and (b) $H_0 R_0 = 0.5$. For distances shorter than the circles, the periodic distribution is unstable, and neighbor rings collapse. The insets show the deformations for these critical distances and a ring force f_r of $3 \frac{\kappa}{R_0}$.

$$f_r \equiv 2\pi\tau_L = \frac{4\pi\kappa\Delta}{R_0} \sqrt{2(1 - R_0 H_0)}. \quad (5)$$

Therefore, within the uncertainty in the value of the shape parameter $0 < R_0 H_0 < 1$, and the values of R_0 and κ given above, we get an upper bound for the required force $f_r \leq 20$ pN to get the observed relative deformation $\Delta \approx 0.2$. The possible nonlinear effects do not change this estimation since they are relatively important only for $R_0 H_0 \lesssim 1$, where the predicted force is well below the linear upper bound (see Appendix A).

This upper estimate for the required force of the Z rings observed in Ref. [10] remains below the estimation of the ring force, $f_r \approx 50$ pN, obtained from the quantitative analysis of AFM images [4,11] and based on the lateral attractive interactions between FtsZ filaments. This theoretical assumption provides a simple and robust explanation for very different *in vitro* experimental results: the formation and aspect of the planar spiral structures (with a typical radius of $0.1 \mu\text{m}$) observed by AFM on mica, and the formation of constricting rings on the tubular liposomes (with radius $\sim 2 \mu\text{m}$). We cannot rule out the possible effects of a spontaneous curvature of the filaments, proposed in Refs. [2,3] as a driving force for the constriction of the membrane, and more experimental evidence would be needed to solve this question. Nevertheless, the lateral interactions are certainly needed to explain the presence of condensed Z rings, instead of open helical structures [5,15], and they should contribute to the constriction of the membranes with any radius.

We address now the possible *in vivo* effects of the Z rings in bacteria, taking into account the important differences with the *in vitro* tubular liposomes (see Appendix C). First of all, the inner bacterial bilayer membrane is a hundred times thinner, and therefore a hundred times less rigid than the multilamellar wall of the liposomes in Ref. [10]. Therefore, the same radial force which produces small deformation of those tubular structures should be enough to produce the full constriction of the bacterial membrane.

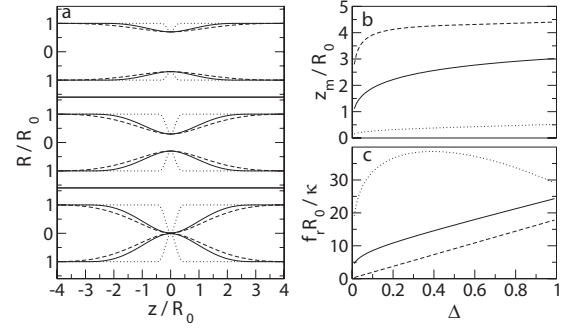


FIG. 3. (a) Shape of the deformed bacterial membrane for $\Delta = 0.3, 0.7$ and 0.99 . (b) Extent of the deformation z_m and (c) the required force f_r . Shown are the results for $\xi = 0.5, \Delta\tilde{p} = 0$ (continuous line), $\xi = 0.01, \Delta\tilde{p} = 0$ (dashed line), and $\xi = 0.5, \Delta\tilde{p} = 1563$ (dotted line, scaled by a factor 10^{-2}).

Another difference is that the elastic bacterial membrane is inside a rigid external wall. The interaction between the inner membrane and the outer wall in rodlike bacteria involves a large number of specific proteins in a very complex scenario that involves both the steady growth of the bacteria along its long axis and its division when it reaches the critical size. There are attempts to incorporate these effects into simplified physical models [16], but the comparison with *in vivo* experimental results is much more difficult and uncertain than for the simpler biomimetic systems analyzed here. In the context of the present work, we may ask for the possible effects of the external wall under the simplest hypothesis, assuming that the wall imposes the boundary condition $R(z) \leq R_w \approx 0.5 \mu\text{m}$. Since R_w is much smaller than the equilibrium radius R_0 produced by the spontaneous mean curvature H_0 in Eq. (1), we may assume $H_0 = 0$ without qualitative changes in the following discussion. The relevant dimensionless parameter becomes here $\xi = 1/2 - R_w^2 \sigma / \kappa$, which goes to zero in the limit when the rigid wall becomes equal to the equilibrium cylindrical radius. We expect to be far from that limit and hence $\xi \lesssim 1/2$. The qualitative difference with the free tubular deformation is that now the perturbation produced by a force ring at $z=0$ is limited to a finite region $|z| \leq z_m$ and, within the linear analysis, corresponds to the solution of the inhomogeneous equation

$$\frac{\partial^4 U(\tilde{z})}{\partial \tilde{z}^4} + \xi \frac{\partial^2 U(\tilde{z})}{\partial \tilde{z}^2} + U(\tilde{z}) = \xi, \quad (6)$$

and the boundary conditions $U(0) = \Delta$, and $U(z_m) = U'(z_m) = 0$. Minimization of the free-energy change with respect to z_m gives the relation between the ring force, f_r , the ring radius, R_r , and the deformation lateral extent, z_m .

Figure 3(a) presents the deformation of the membrane for extremal values of ξ and several relative deformations, up to $\Delta = 1$ which gives the complete constriction of the cylindrical membrane. The required force, f_r , and the lateral extent of the membrane deformation, z_m , are presented in Fig. 3(b). Both f_r and z_m grow very rapidly, as $\Delta^{1/4}$, for small deformations (see Appendix C). For larger Δ the deformation extent is nearly saturated at $z_m \approx 4R_w$, while the required force increases linearly up to a maximum value of $\approx 20\kappa/R_0$.

Assuming a bending rigidity $\kappa=20kT$, typical of a single bilayer membrane, and the *E. coli* radius $R_w=0.5 \mu\text{m}$, the maximum required force from Eq. (5) is found to be $f_r \lesssim 4 \text{ pN}$, well below the estimated value for *in vitro* Z rings.

However there is still another qualitative difference between the deformations of cylindrical membranes and that of *E. coli* or other rodlike bacteria during their division. These bacteria keep a large osmotic pressure difference, $\Delta p \approx 4$ atmospheres, between the inner cytoplasm and the external medium [17]. If a volume times Δp term is added to the membrane Hamiltonian, the linear equation for the deformations becomes

$$\frac{\partial^4 U(\tilde{z})}{\partial \tilde{z}^4} + (\xi - \Delta \bar{p}) \frac{\partial^2 U(\tilde{z})}{\partial \tilde{z}^2} + (1 - \Delta \bar{p}) U(\tilde{z}) = \xi, \quad (7)$$

with $\xi = \frac{1}{2} - R_0^2 \frac{\sigma}{\kappa} + \Delta \bar{p}$ and the deformation for a given force depends dramatically on the value of $\Delta \bar{p} = \Delta p R_0^3 / \kappa$. Assuming that the whole $\Delta p = 4 \text{ atm}$ is acting between the interior of the lipidic membrane and the interstitial space between this membrane and the rigid external wall, the *in vitro* estimate of $f_r \approx 50 \text{ pN}$ would produce a fully negligible deformation ($\Delta \approx 10^{-12}$) on the membrane. The drastic reduction in the pressure difference to $\Delta p = 0.01 \text{ atm}$ would produce the deformations and forces shown in Fig. 3. The extent of the deformed segment becomes much shorter and the force increases having now a maximum of $f_r \approx 600 \text{ pN}$ at $\Delta \approx 0.4$.

IV. CONCLUSIONS

The theoretical analysis of very different *in vitro* experiments for FtsZ proteins presented here provides a comprehensive explanation of the deformation of tubular multilamellar liposomes monitored by fluorescence microscopy [10] and of the protein filament structures observed by AFM on mica [12]. The theoretical predictions [4,11,14] are based on the role of the lateral attractive interaction between filaments as the assumed driving force to form condensed aggregates with the form of spiral rolls on planar substrates and rings on cylindrical supports. The same mechanism leads to a robust explanation for the generation of a constricting force in the latter case [4,6,7,14], in the range of 50–100 pN and nearly independent of the cylindrical radius and the ring width. The analysis presented here for the observed deformation of tubular liposomes under *in vitro* formation of FtsZ rings fits well with the order of magnitude of that force and explains the experimentally observed trend for the distribution of rings along cylindrical liposomes.

There are important differences between the modified FtsZ-*mts* protein used in Ref. [10] to get its direct anchoring to the phospholipid membrane and the FtsZ observed by AFM on mica [12]. Any approach between the elements used in these experiments, such as AFM images of FtsZ-*mts* anchored to a phospholipid membrane on a planar substrate, would offer valuable experimental data for a firmer theoretical analysis. Also, a more precise characterization of the tubular liposome deformations, and their dependence with

in vitro factors controlling the polymerization of the FtsZ protein monomers would be very helpful. Nevertheless, we showed that the self-assembled structures of FtsZ in controlled *in vitro* experiments are getting within the range of physical modeling and analysis. The goal of these efforts should be the comprehensive interpretation of the experimental *in vitro* evidence on the basis of the elementary effective interactions between FtsZ monomers.

The physical understanding of the *in vivo* function of the Z ring is much more uncertain. We have shown in this paper that some qualitative aspects, such as the effect of the rigid bacterial wall in its most simplified form, may be explored with the theoretical methods used here. However, the role of the volume constraint and the osmotic pressure difference between the inner lipid membrane and the outer bacterial wall would be crucial for the quantitative analysis of the force required to achieve the bacterial division, and we propose further experimental studies in this line to achieve this purpose. They are related to the active or passive role of the external wall during the different phases of the bacterial growth and division process [17], and at the present stage there is a lack of controlled experimental data on which quantitative physical models can be based.

ACKNOWLEDGMENTS

The authors acknowledge fruitful discussions with F. Monroy. This work was supported by the Dirección General de Investigación of Spain under the Grants No. FIS2007-65869-C03 (I.H. and P.T.) and No. FIS2009-12964-C05-02 (F.C. and A.H.M.) and by the Comunidad Autónoma de Madrid under Grant No. s-0505/ESP-0299 (I.H. and P.T.).

APPENDIX A: DEFORMATION PRODUCED BY A SINGLE FORCE RING

1. Linear analysis

Assuming axial symmetry for the cylindrical liposomes under the effect of a force ring, the tubular shape is described by the radius $R(z)$ taking z along the cylindrical axis. The contributions to the membrane free energy are written in terms of surface tension σ and bending rigidity κ :

$$F_{mem} = \int dA(z) \left[\frac{\kappa}{2} (H(z) - H_0)^2 + \sigma \right], \quad (A1)$$

where H_0 is the spontaneous curvature of the membrane. The differential element of area dA and the mean curvature $H(z)$ are

$$dA(z) = R(z) \sqrt{1 + R'(z)^2} dz, \\ H(z) = \frac{1}{R(z) \sqrt{1 + R'(z)^2}} - \frac{R''(z)}{[1 + R'(z)^2]^{3/2}}. \quad (A2)$$

The equilibrium radius of a cylindrical membrane R_0 is related to the parameters σ, κ and H_0 ,

$$\frac{1}{R_0^2} = H_0^2 + \frac{2\sigma}{\kappa}. \quad (\text{A3})$$

The contribution of the Z ring (r) to the free energy might be thought of as a series of line tensions $\tau(z)$ placed between $z=-\epsilon$ and $z=\epsilon$,

$$F_r = 2\pi \int_{-\epsilon}^{\epsilon} dz [\tau(z) \tilde{R}(z)]. \quad (\text{A4})$$

We use the functions $\tilde{R}(z) = R_0[1 - \tilde{U}(z)]$ to represent the shape of the deformation between $z=-\epsilon$ and $z=\epsilon$, i.e., within the region under the action of the force ring, while we keep $R(z) = R_0[1 - U(z)]$ to represent the region $|z| > \epsilon$ where $\tau(z)$ vanishes. In the limit of $\epsilon \ll R_0$, the only relevant parameter should be the depth of the deformation, $\Delta = \tilde{U}(0) = U(0)$, but allowing for a finite width of the force rings helps to make clear what are the relevant matching conditions between $\tilde{U}(z)$ and $U(z)$ at $z = \pm \epsilon$.

In its quadratic form, the free-energy functional for the membrane deformation can be written like this:

$$\begin{aligned} \Delta F_{mem} = \frac{2\pi\kappa}{R_0} \int dz \left[\frac{U(z)^2}{2} - R_0^2(1 - R_0H_0)U''(z) \right. \\ \left. + R_0^3H_0U(z)U''(z) + R_0^4 \frac{U''(z)^2}{2} \right]. \quad (\text{A5}) \end{aligned}$$

Minimization of the functional ΔF_{mem} gives the deformations $U(z) = 1 - \frac{R(z)}{R_0}$ for $|z| > \epsilon$, while $\tilde{U}(z)$ for $|z| < \epsilon$ has to be obtained from the minimization of $\Delta F_{mem} + \Delta F_r$, to include the effects of the line tension $\tau(z)$.

In terms of the dimensionless variables $\tilde{z} = z/R_0$, $\tilde{\epsilon} = \epsilon/R_0$, and $\tilde{\tau}(\tilde{z}) = R_0\tau(z)/\kappa$, the equations that have to be solved are

$$\begin{aligned} \frac{\partial^4 U(\tilde{z})}{\partial \tilde{z}^4} + 2R_0H_0 \frac{\partial^2 U(\tilde{z})}{\partial \tilde{z}^2} + U(\tilde{z}) = 0, \\ |\tilde{z}| > \tilde{\epsilon}, \quad (\text{A6}) \end{aligned}$$

$$\begin{aligned} \tilde{\tau}(\tilde{z}) + \frac{\partial^4 \tilde{U}(\tilde{z})}{\partial \tilde{z}^4} + 2R_0H_0 \frac{\partial^2 \tilde{U}(\tilde{z})}{\partial \tilde{z}^2} + \tilde{U}(\tilde{z}) = 0, \\ |\tilde{z}| < \tilde{\epsilon}, \quad (\text{A7}) \end{aligned}$$

where the line tension density $\tau(z)$ may be considered as a Lagrange multiplier which is determined by a given shape of $\tilde{U}(z)$.

The matching conditions at $\tilde{z} = \pm \tilde{\epsilon}$ are

$$R_0H_0[\tilde{U}'(\tilde{\epsilon}) - U'(\tilde{\epsilon})] + \tilde{U}'''(\tilde{\epsilon}) - U'''(\tilde{\epsilon}) = 0, \quad (\text{A8})$$

$$R_0H_0[U(\tilde{\epsilon}) - \tilde{U}(\tilde{\epsilon})] + U''(\tilde{\epsilon}) - \tilde{U}''(\tilde{\epsilon}) = 0, \quad (\text{A9})$$

with all the derivatives taken with respect to the dimensionless variable \tilde{z} .

The finiteness of $\tau(z)$ and the assumption of a smooth distribution of the force that goes to 0 as $|z| \rightarrow \epsilon$ make all the derivatives continuous. Far from the force ring, the deforma-

tion vanishes, $U(\tilde{z}) \rightarrow 0$ for large $|\tilde{z}|$, and the general solution of Eq. (A6) for $|\tilde{z}| > \tilde{\epsilon}$ is given by

$$U(\tilde{z}) = - \frac{\Delta \exp(-\zeta^- |\tilde{z}|)}{\cos(\varphi_0)} \cos(\zeta^+ |\tilde{z}| - \varphi_0), \quad (\text{A10})$$

with $\zeta^\pm = \sqrt{(1 \pm R_0H_0)/2}$.

Now we will show that the two remaining parameters, C and φ_0 , are fixed by the value of U and its first derivative at $z=0$. Therefore we will take the limit of vanishing force ring width. Before we can do that, we will use Eqs. (A7)–(A9) to determine the total force exerted by the Z ring which is equal to the integrated line tension density, $\tau(\tilde{z})$ between $\tilde{z} = -\tilde{\epsilon}$ and $\tilde{z} = \tilde{\epsilon}$,

$$\begin{aligned} f_r = 2\pi\tau_L \\ = 2\pi \int_{-\epsilon}^{\epsilon} dz \tau(z) \\ = - \frac{2\pi\kappa}{R_0} \int_{-\epsilon}^{\epsilon} dz [\tilde{U}(\tilde{z}) + 2R_0H_0\tilde{U}''(\tilde{z}) + \tilde{U}'''(\tilde{z})] \\ = - \frac{4\pi\kappa}{R_0} [2R_0H_0\tilde{U}'(\tilde{\epsilon}) + \tilde{U}'''(\tilde{\epsilon})]. \quad (\text{A11}) \end{aligned}$$

$\tilde{U}(\tilde{z})$ has to satisfy the matching conditions Eqs. (A8) and (A9) which imply the equality of \tilde{U} and U at $|\tilde{z}| = \epsilon$ up to the third derivative,

$$\begin{aligned} \tilde{U}(\tilde{\epsilon}) &= U(\tilde{\epsilon}), \\ \tilde{U}'(\tilde{\epsilon}) &= U'(\tilde{\epsilon}), \\ \tilde{U}''(\tilde{\epsilon}) &= U''(\tilde{\epsilon}), \\ \tilde{U}'''(\tilde{\epsilon}) &= U'''(\tilde{\epsilon}). \quad (\text{A12}) \end{aligned}$$

Furthermore, for given $U(\tilde{z})$ and $U'(\tilde{z})$, the subsequent derivatives are fixed. This can be easily seen by splitting up the fourth order differential operator in Eq. (A6), $\partial_z^4 + (2R_0H_0)\partial_z^2 + 1$ into two second-order differential operators, $(\partial_z^2 + 2\zeta^- \partial_z + 1)(\partial_z^2 - 2\zeta^- \partial_z + 1)$, with ζ^- defined after Eq. (A10). The solution of the second-order differential operator with the minus sign grows exponentially, so the only physical solution is the exponentially decaying solution of the second-order differential operator with the plus sign. This operator is associated to the second-order differential equation,

$$\frac{\partial^2 U(\tilde{z})}{\partial \tilde{z}^2} + 2\zeta^- \frac{\partial U(\tilde{z})}{\partial \tilde{z}} + U(\tilde{z}) = 0. \quad (\text{A13})$$

Together with Eqs. (A12), we get for the ring force

$$f_r = \frac{4\pi\kappa}{R_0} [U'(\tilde{\epsilon}) + 2\zeta^- U(\tilde{\epsilon})]. \quad (\text{A14})$$

We take the limit of vanishing ring width, $\epsilon \rightarrow 0$, so that the whole effect of the force ring is set by the depth of the deformation, $\Delta := U(0)$, and we have $U'(0) = 0$ in order to

guarantee a finite value of $U'''(0)$ which is proportional to the ring force Eq. (A11). The matching conditions at $z=0$ are reduced to

$$2U'''(0) = \tilde{\tau}_L = \frac{\tau_L R_0}{\kappa}, \quad (\text{A15})$$

in terms of the total line tension τ_L . The shape of the deformation [Eq. (4)] becomes

$$U(\tilde{z}) = -\frac{\Delta}{\cos(\varphi_0)} \exp(-\zeta^- |\tilde{z}|) \cos(\zeta^+ |\tilde{z}| - \varphi_0), \quad (\text{A16})$$

with $\tan(\varphi_0) = \frac{\zeta^-}{\zeta^+}$.

The generic shape of the deformation is that of a damped oscillation, ζ^- takes values between $\sqrt{2}/2$ and 0 depending on the relative importance of surface tension and spontaneous curvature. For $H_0=0$ the membrane shape equation becomes

$$U(\tilde{z}) = -\sqrt{2}\Delta \exp\left(-\frac{\tilde{z}}{\sqrt{2}}\right) \cos\left(\frac{\pi}{4} - \frac{\tilde{z}}{\sqrt{2}}\right). \quad (\text{A17})$$

Here the period of the cosine is $2\sqrt{2}\pi$. For increasing spontaneous curvature, the period becomes shorter and the decay of the deformation slower. In the limit of vanishing surface tension, $\sigma=0$ ($R_0H_0=1$), the oscillations in $U(z)$ become undamped as a pearling instability of the cylindrical shape. Now the exponential decay vanishes completely and the solution is purely periodic with a period of 2π ,

$$U(\tilde{z}) = -\Delta \cos(\tilde{z}). \quad (\text{A18})$$

Another consequence of taking the limit of vanishing ring width is that the contribution of the Z ring to the free energy can be expressed as

$$F_r = \oint dl \tau. \quad (\text{A19})$$

We can define an effective bending rigidity, κ_{eff} , so that the ring force becomes

$$f_r = \kappa_{\text{eff}} \frac{\Delta}{R_0}, \quad (\text{A20})$$

with $\kappa_{\text{eff}} = 4\pi\kappa\sqrt{2(1-R_0H_0)}$.

2. Beyond the linear analysis

The solutions that we have found for the shape of a liposome deformed by a force ring and for the deformation depth that is attained for a certain force are valid for small relative deformations. The result of the minimization of the membrane free-energy functional is a highly nonlinear fourth order differential equation that has to be solved in order to obtain the membrane shape $R(z)$. This might be done numerically using shooting methods, but we have restricted our analysis to the linearized equation which could be solved analytically. In order to get an idea of the validity of this approach, we can calculate an upper limit of the actual required force by its numerical calculation using the shape $R(z)$ determined in the linear analysis,

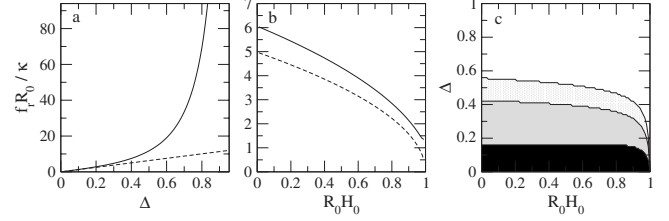


FIG. 4. Force required for (a) a relative deformation Δ of a liposome with spontaneous curvature $R_0H_0=0.5$ and (b) a relative deformation $\Delta=0.28$ of a liposome with spontaneous curvature R_0H_0 . The dashed line is the result of the linear approximation and the continuous line gives an upper bound with nonlinear effects. (c) Relative maximal error in the linear estimation for different values of R_0H_0 and Δ . For parameter pairs within the black (gray, light gray) region, the maximal error is 0.1 (0.5 and 1).

$$f_{r,nl} = -\frac{\partial F_{mem}}{\partial \Delta}. \quad (\text{A21})$$

The ring force depends on two parameters, Δ and R_0H_0 . For fixed R_0H_0 , of course, the error grows for increasing Δ . Figure 4(a) shows $f_{r,nl}$ as an upper bound of the ring force as a function of Δ compared to the result of the linear approximation for $R_0H_0=0.5$. In Fig. 4(b) Δ is fixed to 0.28 and the force is shown as a function of R_0H_0 . For small values of R_0H_0 the possible nonlinear effects do not change significantly the estimated force. The relative error becomes important for $R_0H_0 \leq 1$, close to the pearling instability of the cylindrical shape. Here in the linear estimation, the force vanishes completely whereas the nonlinear upper bound remains finite.

Figure 4(c) reflects the degree of validity of the linear approximation as a function of the spontaneous curvature and the deformation depth. The different levels of gray represent sections with growing maximal error. In summary, the linear analysis gives a reasonable estimation of the deformation force and shape for small deformations up to about 25% and spontaneous curvatures up to about $0.8R_0$.

APPENDIX B: DEFORMATION PRODUCED BY A PERIODIC ROW OF FORCE RINGS

Instead of having one force ring at $z=0$ we set up a periodic distribution of force rings separated by a distance $z_s R_0$ and located at $z = \frac{kz_s}{2}$ with $k = \pm 1, 2, 3, \dots$. So, the new boundary conditions are

$$\begin{aligned} U\left(\pm \frac{kz_s}{2}\right) &= \Delta, \\ U'\left(\pm \frac{kz_s}{2}\right) &= 0, \end{aligned} \quad (\text{B1})$$

taking again the limit of vanishing ring width. Now, the exponentially growing part of the solution of Eq. (A6) will also contribute to the shape of the membrane. We will distinguish between the general case of a membrane with finite surface tension and the limit of $\sigma=0$. For $R_0H_0 < 1$, the membrane shape for $|\tilde{z}| < \frac{z_s}{2}$ can be expressed as

$$U(\bar{z}) = 2\Delta[C^+ \cos(\zeta^+ \bar{z}) \cosh(\zeta^- \bar{z}) + C^- \sin(\zeta^+ \bar{z}) \sinh(\zeta^- \bar{z})], \quad (\text{B2})$$

with

$$C^\pm = \frac{\mp \zeta^\pm \sinh\left(\frac{\zeta^- z_s}{2}\right) \cos\left(\frac{\zeta^+ z_s}{2}\right)}{\zeta^+ \sinh(\zeta^- z_s) + \zeta^- \sin(\zeta^+ z_s)} - \frac{\zeta^\mp \cosh\left(\frac{\zeta^- z_s}{2}\right) \sin\left(\frac{\zeta^+ z_s}{2}\right)}{\zeta^+ \sinh(\zeta^- z_s) + \zeta^- \sin(\zeta^+ z_s)}. \quad (\text{B3})$$

As before, the effective bending rigidity of the membrane is related to the third derivative of U at the location of the force ring,

$$\begin{aligned} \kappa_{\text{eff}}(z_s) &= 4\pi\kappa \frac{U'''(\frac{z_s}{2})}{\Delta} = \frac{4\pi\kappa}{R_0} \sqrt{2(1-R_0 H_0)} \\ &= \frac{\cosh(\zeta^- z_s) - \cos(\zeta^+ z_s)}{\sinh(\zeta^- z_s) + \tan(\varphi_0) \sin(\zeta^+ z_s)}. \end{aligned} \quad (\text{B4})$$

As we have mentioned above, κ_{eff} is a function of the distance between the force rings, z_s . For constant ring force it is related to the membrane free energy through

$$\Delta F_{\text{mem}} = \frac{R_0^2 f_r^2}{2\kappa_{\text{eff}}}. \quad (\text{B5})$$

For vanishing ring separation κ_{eff} approaches zero as it is defined as the effective bending rigidity of the membrane per period. For large values of z_s , the effective bending rigidity reaches the same value as for a single force ring. This is the limit of non interacting rings where the shape of the membrane adopts the form of Eq. (A16) centered at the site of each force ring. Between these two extremes, $\kappa_{\text{eff}}(z_s)$ experiences a series of exponentially decaying maxima and minima for $\sin(\zeta^+ z_s) = 0$,

$$z_s = l\pi \sqrt{\frac{2}{1+R_0 H_0}}, \quad (\text{B6})$$

with $l=1, 2, \dots$. For increasing relative spontaneous curvature the decay becomes less efficient and in the limit of $R_0 H_0 = 1$ it vanishes completely. In this case, κ_{eff} approaches zero for force rings separated by a relative distance of 2π as a consequence of the pearling instability of the cylindrical shape. The membrane free-energy change is represented as a function of the ring separation in Fig. 5(a) for different values of $R_0 H_0$.

For $l=1$, κ_{eff} reaches its maximum. This means that for distances $z_s > z_{\text{max}}$ the separation of the force rings is energetically more favorable than its approach. When we consider a distribution of rings that is limited to a finite tube, the possibility of ring separation is also limited and so the question to ask is whether the periodic distribution is stable. Therefore we imagine two rings at a distance of $z_s - d$ and its neighbor rings at a distance of $z_s + d$. We can calculate an effective bending rigidity $\kappa_{\text{eff}}(z_s, d) = \frac{1}{2}[\kappa_{\text{eff}}(z_s - d) + \kappa_{\text{eff}}(z_s + d)]$. For $z_s = z_{\text{max}}$, $\kappa_{\text{eff}}(z_s, d)$ has a maximum for $d=0$. That means that the periodic distribution is unstable. For a small fluctuation in the periodicity, two

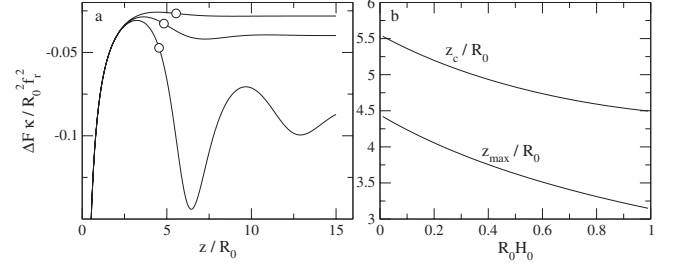


FIG. 5. (a) Free energy change in a liposome membrane with a periodic distribution of Z rings as a function of the ring separation for $R_0 H_0 = 0$ (upper line), $R_0 H_0 = 0.5$ (middle line), and $R_0 H_0 = 0.9$ (lower line). (b) Distance z_{max} between periodically distributed force rings where the free-energy change in the liposome has its maximum. For ring separations shorter than z_c [circles in (a)] the periodic distribution is unstable and neighbor rings collapse.

neighbor rings will enter into the attractive part of the effective potential and collapse. We have to search for the critical distance z_c where $\kappa_{\text{eff}}(z_s, d)$ has a minimum for $d=0$. We obtain z_c by solving the transcendental equation

$$\tan(\zeta^+ z_c) = \frac{\zeta^- \sinh(\zeta^- z_c)}{\zeta^+ \cosh(\zeta^- z_c)}, \quad z_c > z_{\text{max}}. \quad (\text{B7})$$

For relative spontaneous curvatures well below one, Eq. (B7) can be approximated by

$$z_c = z_{\text{max}} \left(\frac{3}{2} - \frac{\varphi_0}{\pi} \right). \quad (\text{B8})$$

Figure 5(b) shows this critical distance as well as z_{max} as a function of the relative spontaneous curvature. The decreasing values for growing $R_0 H_0$ reflect the decreasing period length in the damped harmonic oscillation of the membrane shape produced by a single force ring.

In summary we can state that rings formed at small distances feel an effective attractive potential and collapse until leaving a periodic distribution with distances greater than $\approx 4.5 - 5.5 R_0$, depending on $R_0 H_0$. For z_s values between the maximum of the free-energy change and the critical distance z_c the effective attraction between the rings results from the instability of the periodic distribution. If the distance between one ring and its right and left neighbors are $z_s + d$ and $z_s - d$, then the free-energy change has a minimum for $d=0$ only for $z_s > z_c$.

APPENDIX C: DEFORMATIONS WITHIN A RIGID WALL

When surrounded by a rigid wall, the radius of the membrane is limited to $R(z) \leq R_w$. A measure for the difference between R_w and the equilibrium radius of the membrane R_0 is given by the parameter ξ ,

$$\xi = \frac{1}{2} - R_w^2 \frac{\sigma}{\kappa} - \frac{1}{2} R_w^2 H_0^2 + \Delta \bar{p}, \quad (\text{C1})$$

with $\Delta \bar{p} = \Delta p R_0^3 / \kappa$. Here we have also added a volume times Δp term, $F_{\text{osm}} = -\int dV(z) \Delta p$, to the membrane free energy in order to take account of the osmotic pressure difference be-

tween the interior of the bacterial cell and the external medium. ξ vanishes for $R_w=R_0$ and it increases with growing difference between R_w and R_0 . The linearized shape equation becomes

$$\frac{\partial^4 U(\tilde{z})}{\partial \tilde{z}^4} + \beta \frac{\partial^2 U(\tilde{z})}{\partial \tilde{z}^2} + \alpha U(\tilde{z}) = \xi, \quad (\text{C2})$$

with $\alpha=1-\Delta\tilde{p}$ and $\beta=\xi+2H_0R_0-\Delta\tilde{p}$, choosing H_0R_0 and $\Delta\tilde{p}$ as independent parameters. The deformed radius, $R(z)$ cannot exceed R_w at any point along the cylinder. This implies a change in the boundary conditions that limits the deformation to a finite range, $|\tilde{z}| < z_m$,

$$U(0) = \Delta,$$

$$U'(0) = U(\pm z_m) = U'(\pm z_m) = 0. \quad (\text{C3})$$

As before, we assume an infinitesimal force ring width. At $|\tilde{z}|=z_m$ the membrane exerts a force proportional to $U'''(\pm z_m)$ that is counterparted by the cell wall. Due to the constraint $U'(\pm z_m)=0$ this force remains finite. The general solution of Eq. (C2) for $\Delta\tilde{p} \neq 1$ and $\beta^2 \neq 4(1-\Delta\tilde{p})$ is

$$U(\tilde{z}) = \frac{\xi}{\alpha} + C \exp\left(\pm \sqrt{-\frac{\beta}{2} \pm \frac{1}{2}\sqrt{\beta^2 - 4\alpha\tilde{z}}}\right). \quad (\text{C4})$$

1. $\Delta\tilde{p}=0$

For $\Delta\tilde{p}=0$ and $R_0 > R_w$ we find that $\beta^2 - 4 < 0$ for all possible values of $R_w H_0$ and $\frac{\sigma}{\kappa}$ and so the shape of the deformation for $|\tilde{z}| < z_m$ is

$$U(\tilde{z}) = \xi - (\Delta + \xi) \cos(\zeta^+ \tilde{z}) \cosh(\zeta^- \tilde{z}) + C_1 \sin(\zeta^+ \tilde{z}) \sinh(\zeta^- \tilde{z}) + C_2 \left[\sin(\zeta^+ \tilde{z}) \cosh(\zeta^- \tilde{z}) - \frac{\zeta^+}{\zeta^-} \cos(\zeta^+ \tilde{z}) \sinh(\zeta^- \tilde{z}) \right], \quad (\text{C5})$$

with

$$\zeta^\pm = \sqrt{\frac{1}{2} \pm \frac{\beta}{4}} \quad (\text{C6})$$

and

$$C_1 = (\Delta + \xi) \frac{\zeta^+ \zeta^-}{\lambda} [\cos(2\zeta^+ z_m) - \cosh(2\zeta^- z_m)] + \frac{2\xi}{\lambda} [\sin(\zeta^+ z_m) \sinh(\zeta^- z_m)],$$

$$C_2 = \frac{(\Delta + \xi) \zeta^-}{\lambda} [\zeta^- \sin(2\zeta^+ z_m) + \zeta^+ \sinh(2\zeta^- z_m)] + \frac{2\xi \zeta^-}{\lambda} [\zeta^- \cosh(\zeta^- z_m) \sin(\zeta^+ z_m) + \zeta^+ \cos(\zeta^+ z_m) \sinh(\zeta^- z_m)],$$

$$\lambda = 1 - (\zeta^-)^2 \cos(2\zeta^+ z_m) - (\zeta^+)^2 \cosh(2\zeta^- z_m). \quad (\text{C7})$$

The coefficients C_1 and C_2 still contain Δ and z_m . In principle, their relation is given by fixing Δ and searching for the

minimum of the membrane free energy with respect to z_m . But, actually, the membrane free energy has no local minimum for z_m , the minimum is of global nature as z_m is found to be just at the limit between deformations that fulfill the condition $R(z) < R_w$ and solutions, where the radius of the membrane exceeds the cell wall. In the latter case, an extra energy term must be added accounting for the infinitely high cost for penetrating the rigid cell wall. The relation between Δ and z_m can be obtained by calculating the minimum of the constriction force for a fixed deformation depth with respect to z_m . We have to solve $\frac{\partial}{\partial z_m} \tilde{U}'''(z_m) = 0$ and that leads to

$$\Delta = \xi \frac{[\zeta^- \sin(\zeta^+ z_m) - \zeta^+ \sinh(\zeta^- z_m)]^2}{2\zeta^+ \zeta^- \sin(\zeta^+ z_m) \sinh(\zeta^- z_m)}. \quad (\text{C8})$$

This relation is equal to $\tilde{U}'''(z_m) = 0$. The ring force, as a function of z_m becomes

$$f_r = \frac{4\pi\kappa}{R_w} \tilde{U}'''(0) = \frac{4\pi\kappa\xi}{R_w} \left[\zeta^+ \frac{\cosh(\zeta^- z_m)}{\sin(\zeta^+ z_m)} - \zeta^- \frac{\cos(\zeta^+ z_m)}{\sinh(\zeta^- z_m)} \right]. \quad (\text{C9})$$

2. $\Delta\tilde{p} \gg 1$

For large osmotic pressure differences, we can approximate $\xi \approx \Delta\tilde{p}$ and the shape equation becomes

$$U(\tilde{z}) = -1 + C_1^+ \sin(\zeta^- \tilde{z}) + C_1^- \sinh(\zeta^- \tilde{z}) + C_2^+ \cos(\zeta^+ \tilde{z}) + C_2^- \cosh(\zeta^+ \tilde{z}), \quad (\text{C10})$$

with

$$\zeta^\pm = \sqrt{R_0 H_0 \pm \sqrt{R_0^2 H_0^2 - 1 + \Delta\tilde{p}}} \approx (\Delta\tilde{p})^{1/4} =: \zeta \quad (\text{C11})$$

and

$$\lambda C_1^\pm = \pm \{ [1 - \cosh(\zeta z_m)] \sin(\zeta z_m) \} \pm \{ [1 - \cos(\zeta z_m)] \sinh(\zeta z_m) \} \pm \Delta [\cosh(\zeta z_m) \sin(\zeta z_m) + \cos(\zeta z_m) \sinh(\zeta z_m)],$$

$$\lambda C_2^\pm = [1 \pm \cos(\zeta z_m)] [1 \mp \cosh(\zeta z_m)] \pm \sin(\zeta z_m) \sinh(\zeta z_m) \pm \Delta [\cos(\zeta z_m) \cosh(\zeta z_m) \mp \sin(\zeta z_m) \sinh(\zeta z_m)] \lambda = 2[1 - \cos(\zeta z_m) \cosh(\zeta z_m)]. \quad (\text{C12})$$

The deformation extent and the ring force are now, respectively,

$$\Delta = 1 - \frac{\sinh(\zeta z_m) \sin(\zeta z_m)}{\cosh(\zeta z_m) - \cos(\zeta z_m)},$$

$$f_r = \frac{4\pi\kappa}{R_w} \Delta \tilde{p}^{3/4} \frac{\cosh(\zeta z_m) \sin(\zeta z_m) - \cos(\zeta z_m) \sinh(\zeta z_m)}{\cosh(\zeta z_m) - \cos(\zeta z_m)}. \quad (\text{C13})$$

3. Small deformations far from equilibrium

In all cases, for deformations of a membrane far from equilibrium ($\xi \gg 0$), both the deformation extent, z_m , and the deformation force, f_r , grow like $\Delta^{1/4}$,

$$z_m = \sqrt{6} \left[\frac{2\Delta}{\xi} \right]^{1/4} \quad (\text{C14})$$

$$f_r = \frac{8\pi\kappa}{R_w} \frac{(2\xi)^{3/4}}{\sqrt{3}} \Delta^{1/4}. \quad (\text{C15})$$

-
- [1] E. Callaway, *Nature (London)* **451**, 124 (2008).
 [2] B. Ghosh and A. Sain, *Phys. Rev. Lett.* **101**, 178101 (2008).
 [3] J. Allard and E. Cytrynbaum, *Proc. Natl. Acad. Sci. U.S.A.* **106**, 145 (2009).
 [4] I. Hörger, E. Velasco, J. Mingorance, G. Rivas, P. Tarazona, and M. Vélez, *Phys. Rev. E* **77**, 011902 (2008).
 [5] I. Hörger, E. Velasco, G. Rivas, M. Vélez, and P. Tarazona, *Biophys. J.* **94**, L81 (2008).
 [6] G. Lan, B. Daniels, T. Dobrowsky, D. Wirtz, and S. Sun, *Proc. Natl. Acad. Sci. U.S.A.* **106**, 121 (2009).
 [7] G. Lan, A. Dajkovic, D. Wirtz, and S. Sun, *Biophys. J.* **95**, 4045 (2008).
 [8] R. Shlomovitz and N. Gov, *Phys. Biol.* **6**, 046017 (2009).
 [9] H. Erickson, *Proc. Natl. Acad. Sci. U.S.A.* **106**, 9238 (2009).
 [10] M. Osawa, D. Anderson, and H. Erickson, *Science* **320**, 792 (2008).
 [11] A. Paez, P. Mateos-Gil, I. Hörger, J. Mingorance, G. Rivas, M. Vicente, M. Velez, and P. Tarazona, *PMC Biophysics* **2**, 8 (2009).
 [12] J. Mingorance, M. Tadros, M. Vicente, J. Gonzalez, G. Rivas, and M. Velez, *J. Biol. Chem.* **280**, 20909 (2005).
 [13] W. Helfrich, *Z. Naturforsch. C* **28**, 693 (1973).
 [14] A. Paez, P. Tarazona, P. Mateos-Gil, and M. Vélez, *Soft Matter* **5**, 2625 (2009).
 [15] S. Andrews and A. Arkin, *Biophys. J.* **93**, 1872 (2007).
 [16] G. Lan, C. Wolgemuth, and S. Sun, *Proc. Natl. Acad. Sci. U.S.A.* **104**, 16110 (2007).
 [17] A. Koch, *Bacterial Growth and Form* (Chapman and Hall, London, 1995).